HALF-LATTICE PATHS AND VIRASORO CHARACTERS

OLIVIER B.-FOURNIER, PIERRE MATHIEU, AND TREVOR A WELSH

ABSTRACT. We first briefly review the role of lattice paths in the derivation of fermionic expressions for the $\mathcal{M}(p, p')$ minimal model characters of the Virasoro Lie algebra. We then focus on the recently introduced half-lattice paths for the $\mathcal{M}(p, 2p \pm 1)$ characters, reformulating them in such a way that the two cases may be treated uniformly. That the generating functions of these half-lattice paths are indeed $\mathcal{M}(p, 2p \pm 1)$ characters is proved by describing weight preserving bijections between them and the corresponding RSOS lattice paths. Here, the $\mathcal{M}(p, 2p - 1)$ case is derived for the first time. We then apply the methods of Bressoud and Warnaar to these half-lattice paths to derive fermionic expressions for the Virasoro characters $\chi_{1,2}^{p,2p\pm1}$ that differ from those obtained from the RSOS paths.

This work is an extension of that presented by the third author at the "7th International Conference on Lattice Path Combinatorics and Applications", Siena, Italy, July 2010.

1. INTRODUCTION

In this work, we are concerned with the development and exploitation of combinatorial models for certain q-series of importance in mathematical-physics. Specifically, we describe various sets of weighted lattice paths, the generating functions of which are the minimal model Virasoro characters $\chi_{r,s}^{p,p'}$, where p and p' are coprime with $1 < p < p'$, $1 \le r < p$ and $1 \le s < p'$. Explicit expressions for these characters are given by

$$(1) \qquad \chi_{r,s}^{p,p'} = \frac{1}{(q)_\infty} \sum_{\lambda=-\infty}^{\infty} (q^{\lambda^2 pp' + \lambda(p'r - ps)} - q^{(\lambda p + r)(\lambda p' + s)}),$$

where $(q)_\infty = \prod_{i=1}^{\infty}(1 - q^i)$.

One motivation for developing such lattice path models is that they may be combinatorially manipulated to produce physically significant *fermionic* expressions [18] for the characters $\chi_{r,s}^{p,p'}$. These expressions may be interpreted as a sum over the energies of the excited states of a system of particles for which identical particles are forbidden to occupy the same states. The following are examples of such expressions:

$$(2a) \qquad \chi_{1,2}^{2,5} = \sum_{n=0}^{\infty} \frac{q^{n^2}}{(q)_n}, \qquad\qquad \chi_{1,2}^{3,7} = \sum_{n_1=0}^{\infty} \sum_{n_2=0}^{\infty} \frac{q^{(n_1+n_2)^2+2n_2^2}}{(q)_{n_1}(q)_{2n_2}},$$

$$(2b) \qquad \chi_{1,3}^{3,4} = \sum_{n=0}^{\infty} \frac{q^{2n^2+2n}}{(q)_{2n+1}}, \qquad\qquad \chi_{1,2}^{4,7} = \sum_{n_1=0}^{\infty} \sum_{n_2=0}^{\infty} \frac{q^{(n_1+2n_2)^2+2n_2^2}}{(q)_{2n_1+4n_2}} \begin{bmatrix} n_1 + 2n_2 \\ n_1 \end{bmatrix}_q,$$

where $(q)_n = \prod_{i=1}^{n}(1 - q^i)$ with $(q)_0 = 1$, and $\begin{bmatrix} m \\ n \end{bmatrix}_q$ is the q-binomial defined by $\begin{bmatrix} m \\ n \end{bmatrix}_q = (q)_m (q)_n^{-1} (q)_{m-n}^{-1}$ for $0 \le n \le m$ and 0 otherwise. Such expressions are also of mathematical interest because they provide the "sum sides" of the Rogers-Ramanujan identities (see [1], for example) and many generalisations. Such identities arise in those cases where a product expression is available for $\chi_{r,s}^{p,p'}$. For example, three of the cases (2) have product expressions:

$$\text{(3a)} \qquad \chi^{2,5}_{1,2} = \prod_{\substack{k=1 \\ k \equiv \pm 1 \bmod 5}}^{\infty} \frac{1}{1-q^k}, \qquad\qquad \chi^{3,7}_{1,2} = \prod_{\substack{k=1 \\ k \not\equiv 0, \pm 2, \pm 10, \pm 12, 14 \bmod 28}}^{\infty} \frac{1}{1-q^k},$$

$$\text{(3b)} \qquad \chi^{3,4}_{1,3} = \prod_{\substack{k=1 \\ k \equiv \pm 1, \pm 4, \pm 6, \pm 7 \bmod 16}}^{\infty} \frac{1}{1-q^k}.$$

See [24] for details and references.

The observation [9] that the generating functions of certain weighted lattice paths are the minimal model characters of the Virasoro algebra, emerged from the study of the restricted-solid-on-solid (RSOS) statistical models by Forrester and Baxter [14]. This extended their earlier work with Andrews [2], which dealt with the unitary (ABF) cases, where $p' = p + 1$. Below, in Section 2, we review a reformulation of these paths due to Foda *et al.* [11], which

FIGURE 1. An RSOS path $h \in \mathcal{P}^{4,9}_{8,6}$.
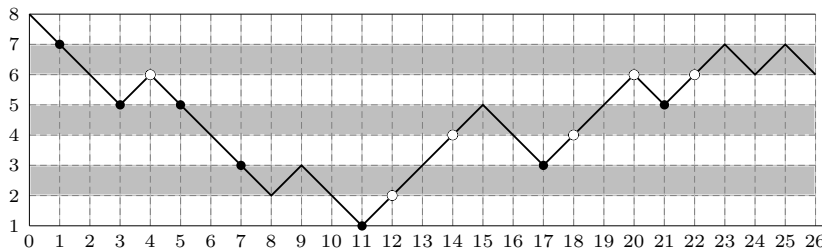
has proved extremely useful in the derivation of fermionic expressions. A typical RSOS path is shown in Fig. 1.

We then describe alternative sets of lattice paths, which have been recently introduced [15, 7], whose generating functions turn out to be Virasoro characters in the non-unitary cases for which $p' = 2p \pm 1$ (the $p' = 2p - 1$ case was sketched in the concluding section of [7]). Significantly, these lattice paths, which we refer to as *half-lattice* paths, share some of the simplifying characteristics of the ABF paths, permitting easier analysis. That the generating functions of these half-lattice paths are Virasoro characters may be proved by formulating weight-preserving bijections between them and the corresponding RSOS paths, the generating functions for which are known to be the $\chi^{p,p'}_{r,s}$ [11]. We describe such bijections in Sections 4 and 5 below.

We then show how these half-lattice paths may be manipulated using the techniques of Bressoud [8] and Warnaar [21] to yield fermionic expressions for their generating functions. Thereupon, through the above bijection, we have obtained fermionic expressions for Virasoro characters $\chi^{p,p'}_{r,s}$ in the cases for which $p' = 2p \pm 1$, $r = 1$ and $s = 2$. These expressions were previously conjectured by Berkovich, McCoy and Pearce [6, §9], and proved by Warnaar [23, §IVD]. We will consider other cases of r and s elsewhere.

A brief review of the Virasoro algebra and its $\mathcal{M}(p, p')$ minimal model representations is given in an appendix. More details may be found in [17, 10].

2. RSOS PATHS

2.1. **Specification.** Here, we define an RSOS path to be an infinite integer sequence $h = (h_0, h_1, h_2, \ldots)$ for which $|h_{x+1} - h_x| = 1$ for each $x \geq 0$. An RSOS path h is said to be (f, g)-restricted if $f \leq h_x \leq g$ for all $x \geq 0$, and b-tailed if there exists L such that $h_x \in \{b, b+1\}$ for $x \geq L$. For p and p' coprime with $1 < p < p'$, and $1 \leq a, b < p'$, define $\mathcal{P}^{p,p'}_{a,b}$ to be the set of those RSOS paths h which are $(1, p' - 1)$-restricted, b-tailed, and have $h_0 = a$.

The *path picture* of an RSOS path $h \in \mathcal{P}_{a,b}^{p,p'}$ is obtained by linking the vertices $(0, h_0)$, $(1, h_1)$, $(2, h_2), \ldots$ on the plane; it has an infinite tail oscillating between adjacent heights b and $b+1$. An example for an RSOS path, its tail truncated, is given in Fig. 1 (the significance of the shading, circles and dots is explained below).

A vertex (x, h_x) is said to be straight if, in the path picture, its two neighbouring edges are in the same direction, and a peak or a valley if those neighbouring edges are in the NE-SE or SE-NE directions respectively.

For $h \in \mathcal{P}_{a,b}^{p,p'}$, it is convenient, for the present purposes, to define $L(h)$ to be the smallest value of $L \in 2\mathbb{Z}$ for which $h_x \in \{b, b+1\}$ for all $x \geq L$.

2.2. Weighting RSOS paths.
When analysing the RSOS paths from $\mathcal{P}_{a,b}^{p,p'}$, it is convenient to shade the horizontal band of the plane between adjacent heights $\lfloor rp'/p \rfloor$ and $\lfloor rp'/p \rfloor + 1$ for each r with $1 \leq r < p$. Such bands are referred to as dark bands, with the others being light bands.

Given a path $h \in \mathcal{P}_{a,b}^{p,p'}$, a vertex (x, h_x) is said to be *scoring* if either it is straight with the right edge in a dark band, or it is not straight with the right edge in a light band, All other vertices are *non-scoring* vertices. Each scoring vertex is designated *up-scoring* or *down-scoring* depending on whether the direction of the left edge is NE or SE respectively. In the path picture, we highlight each up-scoring vertex with an unfilled circle, and each down-scoring vertex with a filled circle. For example, see Fig. 1.

For each vertex (x, h_x) we set

$$(4) \qquad u_x = \frac{1}{2}(x - h_x + a), \qquad v_x = \frac{1}{2}(x + h_x - a).$$

The weight $wt(h)$ of $h \in \mathcal{P}_{a,b}^{p,p'}$ is then defined to be the sum over the up-scoring vertices of their values of u_x, plus the sum over the down-scoring vertices of their values of v_x:

$$(5) \qquad wt(h) = \sum_{\substack{\text{up-scoring} \\ (x,h_x)}} u_x + \sum_{\substack{\text{down-scoring} \\ (x,h_x)}} v_x.$$

For example, on enumerating the scoring vertices of the path h in Fig. 1 from left to right, we obtain $wt(h) = 0 + 0 + 3 + 1 + 1 + 2 + 9 + 9 + 6 + 11 + 11 + 9 + 12 = 74$. This definition of $wt(h)$ is due to Foda *et al.* [11], and is a considerable simplification on that originally given in [14]. Note that $wt(h)$ is finite only if $b = \lfloor rp'/p \rfloor$ for r satisfying $1 \leq r < p$, for otherwise the infinite tail of h lies in a light band, whereupon each of its vertices has a positive contribution to $wt(h)$.

The generating function $X_{a,b}^{p,p'}(q)$ for the set $\mathcal{P}_{a,b}^{p,p'}$ of RSOS paths is then defined by

$$(6) \qquad X_{a,b}^{p,p'}(q) = \sum_{h \in \mathcal{P}_{a,b}^{p,p'}} q^{wt(h)}.$$

It may be shown that if $b = \lfloor rp'/p \rfloor$ then

$$(7) \qquad X_{a,b}^{p,p'}(q) = \chi_{r,a}^{p,p'},$$

where the Virasoro character $\chi_{r,a}^{p,p'}$ is given explicitly in (1). This result was proved in [11] using recurrence relations for the paths. It may also be proved using an inclusion-exclusion argument. Because of this result, the RSOS lattice paths may be used as convenient labels for the states of the minimal model Virasoro modules.

2.3. Obtaining Fermionic expressions.
In those cases for which $p' = p + 1$ (the ABF cases), the weighting rule degenerates to that originally given in [2], where $wt(h)$ is obtained simply by summing half the x positions of the straight vertices of the path h. This weighting rule was necessary for Warnaar [21, 22] to give a direct segmentation of a path, from which fermionic expressions for each $\chi_{r,s}^{p,p+1}$ could be immediately deduced.

Fermionic expressions are not so readily derived in the general $p' > p + 1$ cases. However, a combinatorial means of obtaining a particle description recursively was devised by Foda *et al.* [11], leading to fermionic expressions for $\chi_{r,s}^{p,p'}$ in all cases in which s and r are respectively a Takahashi length and a truncated Takahashi length [13] (these expressions were previously obtained in [3, 5]). These methods were subsequently extended to yield fermionic expressions for all $\chi_{r,s}^{p,p'}$ [24]. An alternative, non-recursive means of obtaining the same particle description in the $p' \geq 2p - 1$ cases was outlined in [16].

3. HALF-LATTICE PATHS

3.1. **Introduction.** Recently, new lattice path models for the minimal models $\mathcal{M}(p, 2p + 1)$ and $\mathcal{M}(p, 2p - 1)$ have been given [15, 7]. The description that follows recasts those descriptions so that the two cases can be treated in a uniform way. To prove that the generating functions in these two cases are the Virasoro characters, we formulate bijections between the half-lattice paths and the corresponding RSOS paths for these minimal models in Sections 4 and 5 respectively. The first of these bijections is a recasting of that described in [7]. The other is new.

3.2. **Specification.** A half-lattice path is defined to be an infinite sequence $\hat{h} = (\hat{h}_0, \hat{h}_{1/2}, \hat{h}_1, \hat{h}_{3/2}, \ldots)$ satisfying $\hat{h}_x \in \frac{1}{2}\mathbb{Z}$ and $|\hat{h}_{x+1/2} - \hat{h}_x| = \frac{1}{2}$ for each $x \in \frac{1}{2}\mathbb{Z}_{\geq 0}$, with the *additional* restriction that if $\hat{h}_x = \hat{h}_{x+1} \in \mathbb{Z}$, then $\hat{h}_{x+1/2} = \hat{h}_x + 1/2$. A half-lattice path $\hat{h}$ is said to be (f, g)-restricted if $f \leq \hat{h}_x \leq g$ for all $x \geq 0$, and $\hat{b}$-tailed if there exists L such that $\hat{h}_x \in \{\hat{b}, \hat{b} + \frac{1}{2}\}$ for $x \geq L$. Here, we define sets of half-lattice paths for each $t \in \frac{1}{2}\mathbb{Z}$ with $t \geq 2$. For $\hat{a}, \hat{b} \in \mathbb{Z}$, define $\mathcal{H}_{\hat{a},\hat{b}}^t$ to be the set of all half-lattice paths $\hat{h}$ that are $(1, t)$-restricted, $\hat{b}$-tailed, with $\hat{h}_0 = \hat{a}$.

The *path picture* of a restricted half-lattice path $\hat{h} \in \mathcal{H}_{\hat{a},\hat{b}}^t$ is obtained by linking the vertices $(0, \hat{h}_0), (1/2, \hat{h}_{1/2}), (1, \hat{h}_1), \ldots$ on the plane; it has an infinite oscillating tail. Examples for $t = 4$ and $t = 7/2$, their tails truncated, are given in Figs. 6 and 12 respectively.

A vertex $(x, \hat{h}_x)$ is said to be a peak, a valley, straight-up or straight-down, depending on whether the pair of edges that neighbour $(x, \hat{h}_x)$ in this path picture are in the NE-SE, SE-NE, NE-NE, or SE-SE directions respectively. In order to likewise specify the nature of the vertex $(0, \hat{a})$ at the path's startpoint, we adopt the convention that $\hat{h}_{-1/2} = \hat{a} + 1/2$. Note that the additional restriction above implies that valleys can only occur at integer heights.

For $\hat{h} \in \mathcal{H}_{\hat{a},\hat{b}}^t$, we define $\hat{L}(\hat{h})$ to be the smallest value of $L \in \mathbb{Z}$ for which $\hat{h}_x \in \{\hat{b}, \hat{b} + \frac{1}{2}\}$ for all $x \geq L$. Then $\hat{h}_{\hat{L}(\hat{h})} = \hat{b}$.

The *unnormalised* weight $\hat{w}^\circ(\hat{h})$ of a half-lattice path $\hat{h}$ is defined to be half the sum of those $x \in \frac{1}{2}\mathbb{Z}_{\geq 0}$ for which $(x, \hat{h}_x)$ is a straight-vertex:

$$(8) \qquad \hat{w}^\circ(\hat{h}) = \frac{1}{2} \sum_{\substack{x \in \frac{1}{2}\mathbb{Z}_{\geq 0} \\ \hat{h}_{x-1/2} \neq \hat{h}_{x+1/2}}} x.$$

The *ground-state path* $\hat{h}^{\mathrm{gs}} \in \mathcal{H}_{\hat{a},\hat{b}}^t$ is defined to be that path which has minimal weight amongst all the elements of $\mathcal{H}_{\hat{a},\hat{b}}^t$ (this path is simply a straight line linking height $\hat{a}$ to $\hat{b}$, followed by a $\hat{b}$-tail). The weight $\widehat{wt}(\hat{h})$ of $\hat{h}$ is then defined by

$$(9) \qquad \widehat{wt}(\hat{h}) = \hat{w}^\circ(\hat{h}) - \hat{w}^\circ(\hat{h}^{\mathrm{gs}}).$$

To illustrate this definition, consider the path $\hat{h} \in \mathcal{H}_{2,4}^5$ which is depicted as the solid line in Fig. 2. Its straight vertices are highlighted here using dots. These are the vertices that

FIGURE 2. Half-lattice path $\hat{h} \in \mathcal{H}_{2,4}^5$ (solid) and $\hat{h}^{gs} \in \mathcal{H}_{2,4}^5$ (dashed)
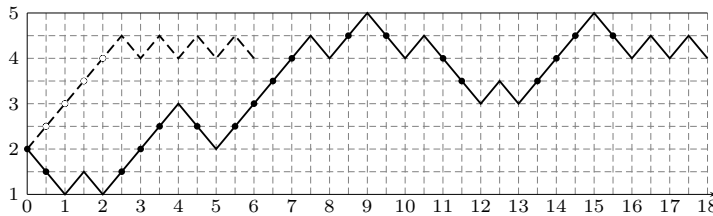
contribute to $\hat{w}^\circ(\hat{h})$ in (8), giving

$$(10) \qquad \begin{aligned} \hat{w}^\circ(\hat{h}) = \tfrac{1}{2}\big(0 + \tfrac{1}{2} + \tfrac{5}{2} + 3 + \tfrac{7}{2} + \tfrac{9}{2} + \tfrac{11}{2} + 6 + \tfrac{13}{2} + 7 + \tfrac{17}{2} \\ + \tfrac{19}{2} + 11 + \tfrac{23}{2} + \tfrac{27}{2} + 14 + \tfrac{29}{2} + \tfrac{31}{2}\big) = \tfrac{137}{2}. \end{aligned}$$

The corresponding ground-state path $\hat{h}^{gs} \in \mathcal{H}_{2,4}^5$ is shown as the dashed line in Fig. 2. Its straight vertices are highlighted here using circles. These lead to

$$(11) \qquad \hat{w}^\circ(\hat{h}^{gs}) = \tfrac{1}{2}\big(\tfrac{1}{2} + 1 + \tfrac{3}{2} + 2\big) = \tfrac{5}{2}.$$

Thereupon (9) yields $\widehat{wt}(\hat{h}) = \tfrac{1}{2}(137 - 5) = 66$.

We define the generating functions for the sets $\mathcal{H}_{\hat{a},\hat{b}}^t$ of half-lattice paths by

$$(12) \qquad Y_{\hat{a},\hat{b}}^t(q) = \sum_{\hat{h} \in \mathcal{H}_{\hat{a},\hat{b}}^t} q^{\widehat{wt}(\hat{h})}.$$

Our first main result is that these generating functions are Virasoro characters:

Theorem 1. *If $t \in \mathbb{Z}_{\geq 2}$, and $\hat{a} \in \{1, 2, \ldots, t\}$ and $\hat{b} \in \{1, 2, \ldots, t-1\}$, then*

$$(13) \qquad Y_{\hat{a},\hat{b}}^t(q) = \chi_{\hat{b},2\hat{a}}^{t,2t+1}.$$

If $t \in \mathbb{Z}_{\geq 2} + \tfrac{1}{2}$, and $\hat{a}, \hat{b} \in \{1, 2, \ldots, t - \tfrac{1}{2}\}$ then

$$(14) \qquad Y_{\hat{a},\hat{b}}^t(q) = \chi_{\hat{a},2\hat{b}}^{t+1/2,2t}.$$

Note that by using the identity (61) we can see that each $\mathcal{M}(p, 2p+1)$ character is one $Y_{\hat{a},\hat{b}}^p(q)$, and each $\mathcal{M}(p, 2p-1)$ character is one $Y_{\hat{a},\hat{b}}^{p-1/2}(q)$. Also note that identity (62) enables Theorem 1 to be simplified by extending (13) to apply to all $t \in \tfrac{1}{2}\mathbb{Z}_{\geq 4}$ since for the non-integer cases of t, (14) is then subsumed into (13).
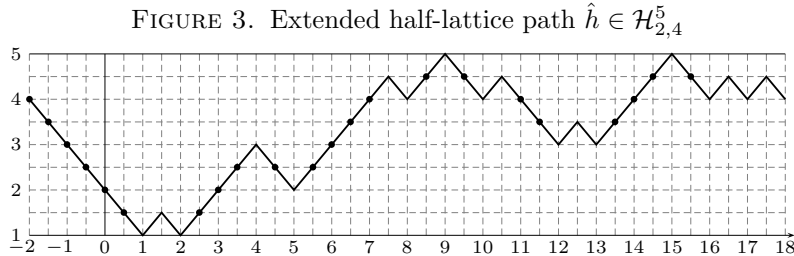
In what follows, Theorem 1 is proved by establishing weight-preserving bijections between the sets of half-lattice paths and the corresponding sets of RSOS paths.

3.3. **Useful trick.** Before we proceed, we describe a useful trick to obtain $\widehat{wt}(\hat{h})$ directly from the path picture of $\hat{h} \in \mathcal{H}_{\hat{a},\hat{b}}^t$. First note that the minimal weight path $\hat{h}^{gs} \in \mathcal{H}_{\hat{a},\hat{b}}^t$ extends between heights $\hat{a}$ and $\hat{b}$ in its first $2e$ (half-integer) steps, where $e = |\hat{a} - \hat{b}|$. An alternative to (9) for obtaining $\widehat{wt}(\hat{h})$, is to extend $\hat{h}$ to the left by $2e$ steps, in such a way that $\hat{h}_{-e} = \hat{b}$ (overriding the above convention for $\hat{h}_{-1/2}$). The renormalised weight $\widehat{wt}(\hat{h})$ is then obtained by summing the x-coordinates of all the straight vertices of this extended path, beginning with its first vertex at $(-e, \hat{b})$, whose nature is specified by setting $\hat{h}_{-e-1/2} = \hat{b} + 1/2$, and dividing by 2.

To illustrate this construction, consider the path $\hat{h} \in \mathcal{H}_{2,4}^5$ represented by the solid line in Fig. 2, for which we found $\widehat{wt}(\hat{h}) = 66$. In this case, the extended path described above

is shown in Fig. 3. From this, the renormalised weight $\widehat{wt}(\hat{h})$ is immediately obtained from its straight vertices via

$$
\begin{aligned}
(15) \quad \widehat{wt}(\hat{h}) = \tfrac{1}{2}\big({} & -2 - \tfrac{3}{2} - 1 - \tfrac{1}{2} + 0 + \tfrac{1}{2} + \tfrac{5}{2} + 3 + \tfrac{7}{2} + \tfrac{9}{2} + \tfrac{11}{2} + 6 + \tfrac{13}{2} \\
& + 7 + \tfrac{17}{2} + \tfrac{19}{2} + 11 + \tfrac{23}{2} + \tfrac{27}{2} + 14 + \tfrac{29}{2} + \tfrac{31}{2} \big) = 66.
\end{aligned}
$$

FIGURE 3. Extended half-lattice path $\hat{h} \in \mathcal{H}_{2,4}^5$


4. THE $\mathcal{M}(p, 2p+1)$ BIJECTION

4.1. **Description.** Here, we describe a weight-preserving bijection

$$
(16) \qquad\qquad \mathcal{P}_{a,b}^{p,2p+1} \leftrightarrow \mathcal{H}_{a/2,b/2}^p,
$$

for $p \geq 2$, and a and b even integers with $1 < a \leq 2p$ and $1 < b < 2p$. From this, via (6), (7) and (12), the identity (13) is immediately established.

Let $h \in \mathcal{P}_{a,b}^{p,2p+1}$, and note that in this case, the RSOS band structure has alternating white and dark bands, with the uppermost and lowermost bands both white. Each pair of adjacent scoring vertices is said to be a particle (for d adjacent scoring vertices, there are $\lfloor d/2 \rfloor$ particles). For the ith such particle of h, counting from the right, let λ_i be the number of non-scoring vertices to its left. If h has n particles, $\lambda = (\lambda_1, \lambda_2, \ldots, \lambda_n)$ is a partition. Now create the path $h^{\mathrm{cut}} \in \mathcal{P}_{a,b}^{p,2p+1}$, by removing all the particles from h, in each case joining up the loose ends, which will be of the same height. In the case of the path from Fig. 1, this yields the path h^{cut} given in Fig. 4, with $\lambda = (9, 8, 5, 1)$.

FIGURE 4. h^{cut} obtained from Fig. 1.
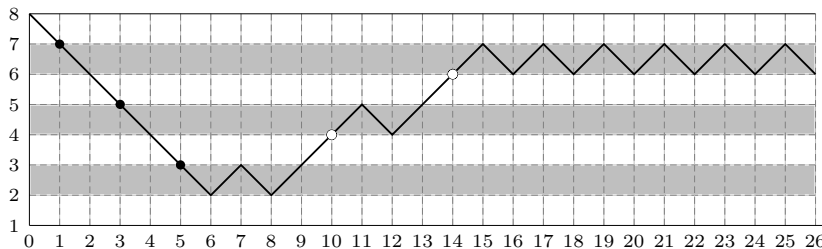
Now obtain the path $\hat{h}^{\mathrm{cut}} \in \mathcal{H}_{a/2,b/2}^p$ by shrinking the path h^{cut} by a factor of two, and discarding the lowermost band, from which the path is necessarily absent. From h^{cut}, we thus obtain the path $\hat{h}^{\mathrm{cut}}$ given in Fig. 5.

Finally, we obtain the bijective image $\hat{h}$ of the original h upon heightening some of the non-integer height peaks of $\hat{h}^{\mathrm{cut}}$, by in each case inserting a NE-SE pair of edges. After setting

$$
(17) \qquad\qquad \mu_i = \lambda_i + n + 1 - i \qquad \text{for} \qquad 1 \leq i \leq n,
$$

the peaks of $\hat{h}^{\mathrm{cut}}$ to be heightened are those numbered $\mu_1, \mu_2, \ldots, \mu_n$ from the left. In the ongoing example, $\mu_1 = 13$, $\mu_2 = 11$, $\mu_3 = 7$ and $\mu_4 = 2$, thereby leading to the half-lattice
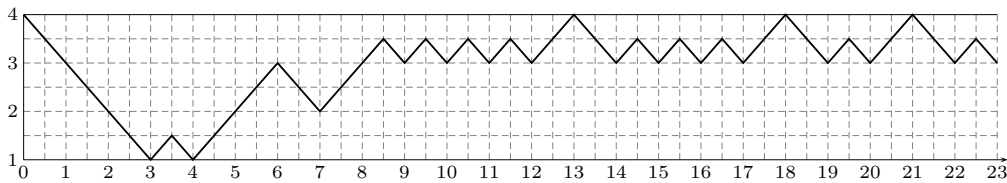
FIGURE 5. Half-lattice path $\hat{h}^{\mathrm{cut}} \in \mathcal{H}_{4,3}^4$ obtained from Fig. 4
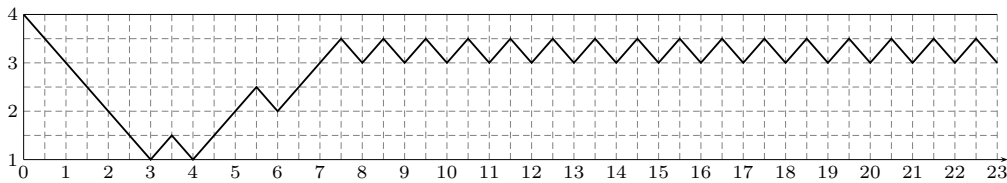
path $\hat{h}$ of Fig. 6. It may be checked that, in this case, $\hat{w}^\circ(\hat{h}) = 297/4$ and $\hat{w}^\circ(\hat{h}^{\mathrm{gs}}) = 1/4$ so that $\widehat{wt}(\hat{h}) = 74$, which equals the weight $wt(h)$ of Fig. 1, as required.

This completes the description of the bijection (16).

FIGURE 6. Half-lattice path $\hat{h} \in \mathcal{H}_{4,3}^4$.

4.2. **Proof of $\mathcal{M}(p, 2p+1)$ bijection.** In what follows, we show that the combined map

$$(18) \qquad h \to (h^{\mathrm{cut}}, n, \lambda) \to (\hat{h}^{\mathrm{cut}}, n, \mu) \to \hat{h}$$

is a weight-preserving bijection between $\mathcal{P}_{a,b}^{p,2p+1}$ and $\mathcal{H}_{\hat{a},\hat{b}}^p$ where we set $\hat{a} = a/2$, $\hat{b} = b/2$, $\lambda = (\lambda_1, \lambda_2, \ldots, \lambda_n)$ and $\mu = (\mu_1, \mu_2, \ldots, \mu_n)$. Note that λ is a partition with at most n parts, and μ, as defined by (17), is a distinct partition with exactly n parts.

That it is a bijection follows because the inverse map from $\mathcal{H}_{\hat{a},\hat{b}}^p$ to $\mathcal{P}_{a,b}^{p,2p+1}$, which is easily described, is well-defined. This relies on the fact that each $\hat{h} \in \mathcal{H}_{\hat{a},\hat{b}}^p$ arises from a unique half-lattice path, $\hat{h}^{\mathrm{cut}}$, whose characteristic property, we recall, is that its peaks are all at non-integer heights; $\hat{h}^{\mathrm{cut}}$ is thus recovered from $\hat{h}$ by shrinking each integer peak. With n the number of such integer peaks, the partition $\mu = (\mu_1, \ldots, \mu_n)$ is determined by setting its parts to be the numberings of the integer peaks amongst all peaks, counted from the left. The parts of μ are necessarily distinct, and thus a genuine partition λ is recovered via (17).

4.3. **Proof of $\mathcal{M}(p, 2p+1)$ weight preservation (i).** The RSOS path h^{cut} is obtained from h by removing the particles numbered $\lambda_1, \lambda_2, \ldots, \lambda_n$. Consider the removal of the ith such particle from h. The number of non-scoring vertices to its left is λ_i. Let k be the total number of scoring vertices in h. The band structure for the $p' = 2p+1$ cases ensures that the first of the two scoring vertices that comprise the particle is necessarily a peak or valley. Let it be at position (x, h_x). If it is a peak, then the following vertex is at $(x+1, h_x - 1)$, and together they contribute

$$(19) \qquad u_x + v_{x+1} = \frac{1}{2}(x - h_x + a + x + 1 + h_x - 1 - a) = x$$

to $wt(h)$. If it is a valley, then the following vertex is at $(x+1, h_x + 1)$, and together they contribute

$$(20) \qquad v_x + u_{x+1} = \frac{1}{2}(x + h_x - a + x + 1 - h_x - 1 + a) = x$$

to $wt(h)$. There are $x - 1 - \lambda_i$ scoring vertices to the left of the particle, and thus $\lambda_i + k - x - 1$ to its right. On removing the particle, the contribution of each of the latter to the weight decreases by one. Thus the total weight reduction on removing the particle is $\lambda_i + k - 1$.

Then, on removing all n of the particles from h, noting that k decreases by two at each step, we obtain

$$
(21) \qquad \begin{aligned}
wt(h^{\mathrm{cut}}) &= wt(h) - \sum_{i=1}^{n} \lambda_i - (k-1) - (k-3) - (k-5) - \cdots - (k-2n-1) \\
&= wt(h) - \sum_{i=1}^{n} \lambda_i - n(k-n).
\end{aligned}
$$

4.4. **Proof of** $\mathcal{M}(p, 2p+1)$ **weight preservation (ii).** The path $h^{\mathrm{cut}} \in \mathcal{P}_{a,b}^{p,2p+1}$ has no neighbouring pair of scoring vertices, which, as is easily seen, implies it has no valleys at odd height, and no peaks at even height. The half-lattice path $\hat{h}^{\mathrm{cut}} \in \mathcal{H}_{\hat{a},\hat{b}}^{p}$, obtained by shrinking h^{cut} by a factor of 2, then has no valleys at non-integer height, and no peaks at integer height. In this section, we show that $\widehat{wt}(\hat{h}^{\mathrm{cut}}) = wt(h^{\mathrm{cut}})$.

First consider the case where $a = b$. On truncating the path h^{cut} after $L(h^{\mathrm{cut}})$ steps, the path then starts and finishes at the same height. We may then match (pair) each path segment with another at the same height, one NE and one SE (the order is immaterial). This matching process is illustrated in Fig. 7.

FIGURE 7. Example of segment matching for a path h.
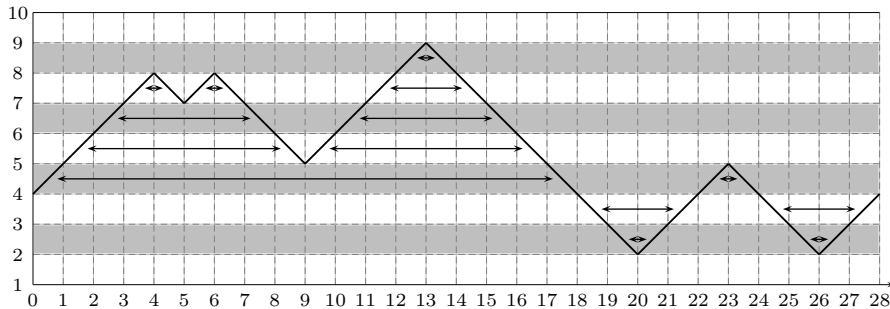
The above restrictions on the peaks and valleys of h^{cut} imply that the scoring vertices of h^{cut} occur at the right ends of all the segments in the light bands. Consider a specific matched pair of segments in a light band, with the left ends of the NE and SE segments at positions (x, y) and $(x', y+1)$ respectively. The two scoring vertices at $(x+1, y+1)$ and $(x'+1, y)$ together contribute

$$
(22) \qquad u_{x+1} + v_{x'+1} = \frac{1}{2}(x + 1 - (y+1) + a + x' + 1 + y - a) = \frac{1}{2}(x + x' + 1)
$$

to $wt(h^{\mathrm{cut}})$.

For the corresponding half-lattice path $\hat{h}^{\mathrm{cut}}$, consider the corresponding matched pair of segments. The four straight vertices at the ends of each of these segments contribute

$$
(23) \qquad \frac{1}{2}\left[\frac{1}{2}x + \frac{1}{2}(x+1) + \frac{1}{2}x' + \frac{1}{2}(x'+1)\right] = \frac{1}{2}(x + x' + 1)
$$

to $\hat{w}^{\circ}(\hat{h}^{\mathrm{cut}})$ (the vertex at $(0, \hat{a})$ will be required here if it is straight). Since this agrees with the contribution (22) of the corresponding two scoring vertices of h^{cut} to $wt(h^{\mathrm{cut}})$, we conclude that $\hat{w}^{\circ}(\hat{h}^{\mathrm{cut}}) = wt(h^{\mathrm{cut}})$. But, for $a = b$, $\widehat{wt}(\hat{h}^{\mathrm{cut}}) = \hat{w}^{\circ}(\hat{h}^{\mathrm{cut}})$, thereby proving that $\widehat{wt}(\hat{h}^{\mathrm{cut}}) = wt(h^{\mathrm{cut}})$ in this $a = b$ case.

In the case that $a \neq b$, we make use of the trick described in Section 3.3 to obtain $\widehat{wt}(\hat{h}^{\mathrm{cut}})$ by extending the path $\hat{h}^{\mathrm{cut}}$ to the left. On the other hand, extending the path h^{cut} to the left by $2e = |a-b|$ steps with $h_{-2e}^{\mathrm{cut}} = b$, creates an RSOS path of unchanged weight $wt(h^{\mathrm{cut}})$ because, via (4), the additional scoring vertices each contribute 0 to the weight. Then, upon

applying the argument used above in the $a = b$ case to these extended paths, we obtain $\widehat{wt}(\hat{h}^{\mathrm{cut}}) = wt(h^{\mathrm{cut}})$ for $a \neq b$ also.

4.5. **Proof of** $\mathcal{M}(p, 2p+1)$ **weight preservation (iii).** Consider a half-lattice path $\hat{h}^{(0)} \in \mathcal{H}^{p}_{\hat{a},\hat{b}}$, having ℓ straight vertices. This count includes consideration of the vertex at $(0, \hat{a})$, which, through the convention stated in Section 3.2, is deemed straight if and only if the first segment of $\hat{h}^{(0)}$ is in the SE direction. The vertices of $\hat{h}^{(0)}$ that do not contribute to its weight are the peaks and valleys. We now determine the change in weight on heightening one of the peaks. Let the peak being heightened be the jth, counting from the left, and let it be situated at $(x, \hat{h}^{(0)}_x)$. There are necessarily j valleys to the left of this peak (perhaps including one at $(0, \hat{a})$), and therefore $2x + 1 - 2j$ straight vertices. After this position, there are thus $\ell - 2x + 2j - 1$ straight vertices. The heightening moves each of these to the right by two (half-integer) positions. It also introduces two straight vertices, at positions $(x, \hat{h}^{(0)}_x)$ and $(x + 1, \hat{h}^{(0)}_x)$. Thus, if this resulting path is denoted $\hat{h}^{(1)}$,

$$
\begin{aligned}
\widehat{wt}(\hat{h}^{(1)}) &= \widehat{wt}(\hat{h}^{(0)}) + \frac{1}{2}(x + (x+1)) + \frac{1}{2}(\ell - 2x + 2j - 1)) \\
&= \widehat{wt}(\hat{h}^{(0)}) + \frac{1}{2}\ell + j.
\end{aligned}
\tag{24}
$$

Note that the heightening increases the value of ℓ by 2. So if we obtain the path $\hat{h}$ by performing a succession of heightenings to a path $\hat{h}^{\mathrm{cut}}$ at peaks numbered $\mu_1, \mu_2, \ldots, \mu_n$, we have

$$
\begin{aligned}
\widehat{wt}(\hat{h}) &= \widehat{wt}(\hat{h}^{\mathrm{cut}}) + \frac{1}{2}(\ell + (\ell+2) + \cdots + (\ell + 2n - 2)) + \sum_{i=1}^{n} \mu_i \\
&= \widehat{wt}(\hat{h}^{\mathrm{cut}}) + \frac{n}{2}(\ell + n - 1) + \sum_{i=1}^{n} \mu_i.
\end{aligned}
\tag{25}
$$

4.6. **Proof of** $\mathcal{M}(p, 2p+1)$ **weight preservation (iv).** Consider the combined map (18). Let k and k' be the number of scoring vertices in h and h^{cut} respectively, and let ℓ be the number of straight vertices. The pair removal process in Section 4.3 shows that $k' = k - 2n$. The matching of edges described in Section 4.5 shows that $\ell = 2k'$ and thus $\ell = 2k - 4n$. Then, using (21) and (25), and the fact that $\widehat{wt}(\hat{h}^{\mathrm{cut}}) = wt(h^{\mathrm{cut}})$, we obtain

$$
\begin{aligned}
\widehat{wt}(\hat{h}) - wt(h) &= \sum_{i=1}^{n} \mu_i - \sum_{i=1}^{n} \lambda_i + \frac{n}{2}(\ell + n - 1) - n(k - n) \\
&= \sum_{i=1}^{n} \mu_i - \sum_{i=1}^{n} \lambda_i - \frac{n}{2}(n + 1) \\
&= 0,
\end{aligned}
\tag{26}
$$

where the final equality follows from (17) because $\sum_{i=1}^{n} \mu_i - \sum_{i=1}^{n} \lambda_i = \sum_{i=1}^{n} i = \frac{1}{2}n(n+1)$. Thus the weight-preserving nature of the bijection (18) has been proved.

5. THE $\mathcal{M}(p, 2p-1)$ BIJECTION

5.1. **Description.** Here, we describe a weight-preserving bijection

$$
\mathcal{P}^{p,2p-1}_{a,b-1} \leftrightarrow \mathcal{H}^{p-1/2}_{b/2,a/2},
\tag{27}
$$

for $p \in \mathbb{Z}_{\geq 3}$, and a and b even integers with $1 < a, b < 2p - 1$. From this, via (6), (7) and (12), the identity (14) is immediately established.

Let $h \in \mathcal{P}^{p,2p-1}_{a,b-1}$, and note that in this case, the RSOS band structure has alternating white and dark bands, with the uppermost and lowermost bands both dark. In this case, particles are identified with pairs of adjacent *non-scoring* vertices [11]. For the ith particle of h, counting from the left, let λ_i be the number of scoring vertices to its right. Due to

the infinite tail, h has an infinite number of such particles with $\lambda_i = 0$ (they form a "Dirac sea"). Let n be the largest value for which $\lambda_n > 0$. Then $\lambda = (\lambda_1, \lambda_2, \ldots, \lambda_n)$ is a partition with exactly n parts. Now create the path $h^{\mathrm{cut}} \in \mathcal{P}_{a,b-1}^{p,2p-1}$ by removing the first n particles from h, in each case joining up the loose ends. To illustrate this, consider the path h given in Fig. 8, for which we find $wt(h) = 112$. Here, $n = 8$ and $\lambda = (12, 12, 11, 11, 8, 4, 4, 2)$. The removal of these first 8 particles yields the path h^{cut} given in Fig. 9.

FIGURE 8. An RSOS path $h \in \mathcal{P}_{6,1}^{4,7}$.
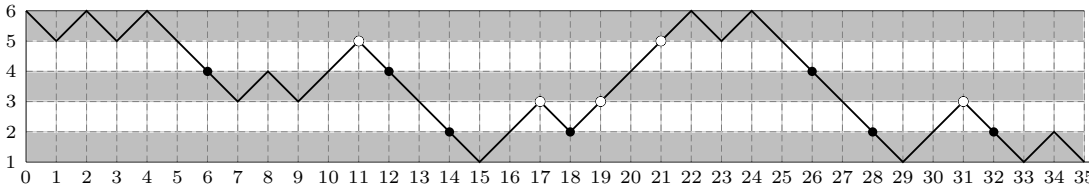
Let k be the total number of scoring vertices in h^{cut} (or h), with m the number of those that are peaks, and define c to be the largest value such that $\lambda_c - c \geq k - m$. Then define the partition $\mu = (\mu_1, \mu_2, \ldots, \mu_c)$ by setting
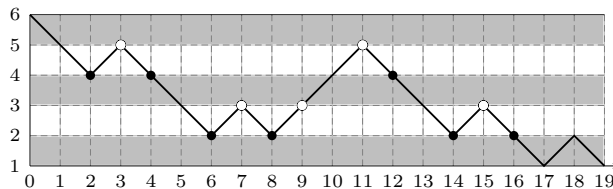
$$(28) \qquad \mu_i = \lambda_i - i - k + m + 1 \qquad \text{for} \qquad 1 \leq i \leq c,$$

and the partition $\nu = (\nu_1, \nu_2, \ldots, \nu_d)$ for $d = n - c$ by setting

$$(29) \qquad \nu_i = \lambda_{i+c} \qquad \text{for} \qquad 1 \leq i \leq d.$$

In the case of the path in Fig. 8, we obtain $k = 12$, $m = 4$, $c = 3$, $\mu = (4, 3, 1)$, $d = 5$ and $\nu = (11, 8, 4, 4, 2)$.

FIGURE 9. $h^{\mathrm{cut}} \in \mathcal{P}_{6,1}^{4,7}$ obtained from Fig. 8

We then create a half-lattice path $\hat{h} \in \mathcal{H}_{b/2,a/2}^{p-1/2}$ from h^{cut} in three stages. Since a, b and $L(h^{\mathrm{cut}})$ are even, it follows that $h_{L(h^{\mathrm{cut}})}^{\mathrm{cut}} = b$. Now form a half-lattice path $\hat{h}^{\mathrm{cut}} \in \mathcal{H}_{b/2,a/2}^{p-1/2}$ by truncating h^{cut} after $L(h^{\mathrm{cut}})$ steps, flipping it horizontally, shrinking it by a factor of two, heightening each peak by $1/2$ unit by inserting a NE-SE edge pair, and finally appending an infinite $(a/2)$-tail. To obtain the band structure for this $t = p - 1/2$ case, we discard the lowermost band that results from this procedure, which is between heights $1/2$ and 1 ($\hat{h}^{\mathrm{cut}}$ doesn't venture there), and append a band between heights $p - 1$ and $p - 1/2$ at the top.

In the case of the path h^{cut} of Fig. 9, note that $L(h^{\mathrm{cut}}) = 16$, whereupon this process yields the path $\hat{h}^{\mathrm{cut}}$ given in Fig. 10.

The half-lattice path $\hat{h}^{\mathrm{int}} \in \mathcal{H}_{b/2,a/2}^{p-1/2}$ is obtained by further heightening some of the peaks in $\hat{h}^{\mathrm{cut}}$ by $1/2$ unit by inserting NE-SE edge pairs. Those that are heightened are the peaks numbered $\mu_1, \mu_2, \ldots, \mu_c$, counting from the left.

In the case of the path $\hat{h}^{\mathrm{cut}}$ of Fig. 10, with $\mu = (4, 3, 1)$, this yields the path $\hat{h}^{\mathrm{int}}$ given in Fig. 11.

For $x \in \mathbb{Z}_{\geq 0}$, the vertex $(x, \hat{h}_x^{\mathrm{int}})$ of $\hat{h}^{\mathrm{int}}$ is designated an *accretion vertex* if neither $(x, \hat{h}_x^{\mathrm{int}})$ nor $(x + 1/2, \hat{h}_{x+1/2}^{\mathrm{int}})$ is a peak. We number these from the right. The path $\hat{h}$ is

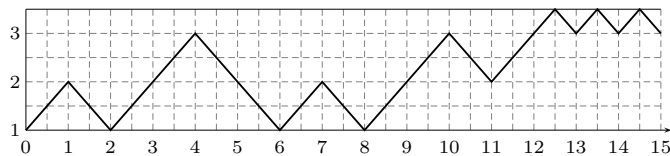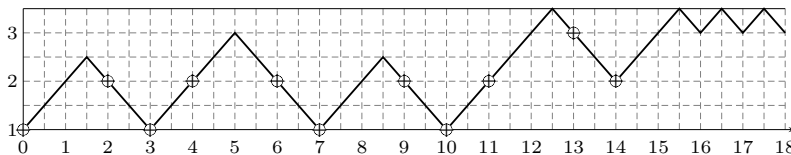FIGURE 10. Half-lattice path $\hat{h}^{\mathrm{cut}} \in \mathcal{H}_{1,3}^{7/2}$ obtained from Fig. 9

FIGURE 11. Half-lattice path $\hat{h}^{\mathrm{int}} \in \mathcal{H}_{1,3}^{7/2}$ obtained from Fig. 10


now obtained from $\hat{h}^{\mathrm{int}}$ by inserting a number of NE-SE edge pairs at each accretion vertex: if $\nu = (\ldots, 3^{f_3}, 2^{f_2}, 1^{f_1})$ in frequency notation, f_j such edge pairs are inserted at the jth accretion vertex.

For the path $\hat{h}^{\mathrm{int}}$ in Fig. 11, each accretion vertex is highlighted using the symbol $\oplus$. With $\nu = (11, 8, 4, 4, 2)$ as above, the insertion process then yields the half-lattice path $\hat{h}$ given in Fig. 12. It may be checked that $\hat{w}^{\circ}(\hat{h}) = 229/2$ here. Then, since $\hat{w}^{\circ}(\hat{h}^{\mathrm{gs}}) = 5/2$, we obtain $\widehat{wt}(\hat{h}) = 112$. As required, this equals the weight $wt(h)$ of the RSOS path h in Fig. 8.

That the map $h \mapsto \hat{h}$ described above is a weight-preserving bijection between the sets (27) is shown below.

FIGURE 12. Half-lattice path $\hat{h} \in \mathcal{H}_{1,3}^{7/2}$ obtained from Fig. 11
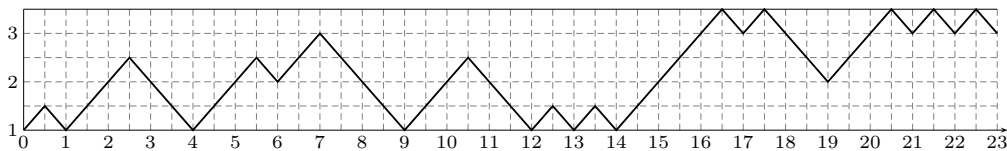
5.2. **Proof of $\mathcal{M}(p, 2p-1)$ bijection.** In what follows, we show that the combined map

$$(30) \qquad h \to (h^{\mathrm{cut}}, n, \lambda) \to (\hat{h}^{\mathrm{cut}}, c, \mu, d, \nu) \to (\hat{h}^{\mathrm{int}}, d, \nu) \to \hat{h}$$

is a weight-preserving bijection between $\mathcal{P}_{a,b-1}^{p,2p-1}$ and $\mathcal{H}_{\hat{a},\hat{b}}^{p-1/2}$, where we set $\hat{a} = b/2$ and $\hat{b} = a/2$. To demonstrate the bijective property, it is sufficient to demonstrate that the inverse of each step in (30) is well-defined.

For the first step, h is recovered from $(h^{\mathrm{cut}}, n, \lambda)$ simply by, for each $i \leq n$, inserting a NE-SE or SE-NE pair of edges at the scoring vertex $\lambda_i + 1$ numbered amongst all the scoring vertices of h^{cut} counted from the right. The pair of edges is chosen so that they lie in a dark band. If λ_i is equal to the total number of scoring vertices in h^{cut}, then a SE-NE edge pair is inserted at the path startpoint $(0, a)$.

The inverse of the second step is achieved by truncating $\hat{h}^{\mathrm{cut}}$ at position $\hat{L}(\hat{h}^{\mathrm{cut}})$ reducing each peak in height by $1/2$ unit by removing a NE-SE edge pair, then flipping the path horizontally, and appending a $(b-1)$-tail. The values of m and k may then be recovered from the resulting h^{cut}, whereupon λ may be recovered from μ and ν using (28) and (29), with $n = c + d$.

The characteristic property of $\hat{h}^{\text{cut}}$ is that, to the left of position $\hat{L}(\hat{h}^{\text{cut}})$, every peak and valley is at integer height. The characteristic property of $\hat{h}^{\text{int}}$ is that, to the left of position $\hat{L}(\hat{h}^{\text{int}})$, every valley is at integer height, while every peak, although not necessarily at integer height, has its two neighbouring vertices both straight. Therefore, for the inverse of the third step, $(\hat{h}^{\text{cut}}, c, \mu)$ is recovered from $\hat{h}^{\text{int}}$ by reducing each non-integer height peak by $1/2$ unit by removing a NE-SE edge pair, and recording their positions $\mu_1, \mu_2, \ldots$ amongst the peaks of $\hat{h}^{\text{int}}$, numbered from the left.

For the fourth step, note that the insertion of a NE-SE edge at an accretion vertex of $\hat{h}^{\text{int}}$ produces a new peak at non-integer height for which the neighbouring two vertices are not both straight. Since $\hat{h}^{\text{int}}$ has no peaks of this nature, $\hat{h}^{\text{int}}$ is thus recovered from $\hat{h}$ by removing the NE-SE edge pairs about each non-integer height peak whose neighbouring vertices are not both straight. The partition ν is then recovered by noting at which accretion vertices of $\hat{h}^{\text{int}}$, numbered from the right, these edge pairs have been removed.

5.3. **Proof of** $\mathcal{M}(p, 2p-1)$ **weight preservation (i).** The RSOS path h^{cut} is obtained from h by removing the particles numbered $\lambda_1, \lambda_2, \ldots, \lambda_n$. Consider the removal of the ith such particle from h. The number of scoring vertices to its right is λ_i. On removing the particle, the coordinates (u_x, v_x) of each scoring vertex to its right are reduced to $(u_x - 1, v_x - 1)$. Therefore, from (5), we see that this removal reduces the weight by λ_i.

Repeating this process for each of the n particles in h then shows that

$$(31) \qquad wt(h^{\text{cut}}) = wt(h) - \sum_{i=1}^{n} \lambda_i.$$

5.4. **Proof of** $\mathcal{M}(p, 2p-1)$ **weight preservation (ii).** Obtain the half-lattice path $\hat{h}^{\text{cut}} \in \mathcal{H}_{\hat{a},\hat{b}}^{p-1/2}$ from $h^{\text{cut}} \in \mathcal{P}_{a,b-1}^{p,2p-1}$ as described above. In this section, we show that $\widehat{wt}(\hat{h}^{\text{cut}}) = wt(h^{\text{cut}})$.

To do this, first regard the path h^{cut}, truncated after $L(h^{\text{cut}})$ steps, as a sequence of lines alternating between the SE and NE directions. The $\mathcal{M}(p, 2p-1)$ band structure, that a and b are even, and the fact that the truncated h^{cut} has no two neighbouring non-scoring vertices implies that each line is of odd length except the first if in the SE direction, and the last if in the NE direction. The odd length lines are of length $2k'-1$ for $k' > 0$ and contain exactly k' scoring vertices, if we include the final vertex, and exclude the first vertex. The possible even length lines are of length $2k'$ for $k' > 0$ and also contain exactly k' scoring vertices. After flipping the path, and heightening the peaks to produce the truncated $\hat{h}^{\text{cut}}$, each of the odd length lines gives rise to a line of length k' which contains $2k'-1$ straight vertices, and the possible even length lines give rise to a line of length k' which contains $2k'$ straight vertices (including consideration of $(0, \hat{a})$). Because of this, we may naturally associate each edge on a line of the truncated h^{cut} with a straight vertex on the corresponding line of the truncated $\hat{h}^{\text{cut}}$: associate the ith edge from the left on the former with the ith straight vertex from the right on the latter.

Through this association, we see that if an edge of h^{cut} is in the SE (resp. NE) direction, then the number of up-scoring (resp. down-scoring) vertices to its right, is equal to half the number of SE (resp. NE) edges to the left of the corresponding vertex in $\hat{h}^{\text{cut}}$, and to the right of $(0, \hat{a})$. This will be used to prove that $\widehat{wt}(\hat{h}^{\text{cut}}) = wt(h^{\text{cut}})$, once we have described alternative means of obtaining the two weights.

In the case of a half-lattice path $\hat{h} \in \mathcal{H}_{\hat{a},\hat{b}}^{t}$, for each vertex $(x, \hat{h}_x)$, we define

$$(32) \qquad \hat{u}_x = \frac{1}{2}(x - \hat{h}_x + \hat{a}), \qquad \hat{v}_x = \frac{1}{2}(x + \hat{h}_x - \hat{a}),$$

in analogy with (4). Note that $\hat{u}_x$ (resp. $\hat{v}_x$) is then half the number of SE (resp. NE) edges between $(0, \hat{a})$ and $(x, \hat{h}_x)$ in $\hat{h}$. Thus $\hat{u}_x$ and $\hat{v}_x$ are the numbers of up-scoring and down-scoring vertices considered in the previous paragraph.

For any RSOS path h, define

$$(33) \qquad w_x = \begin{cases} \text{number of up-scoring vertices to right of } (x, h_x) & \text{if } h_x = h_{x-1} - 1, \\ \text{number of down-scoring vertices to right of } (x, h_x) & \text{if } h_x = h_{x-1} + 1, \end{cases}$$

for all $x > 0$. Since the contribution of an up-scoring (resp. down-scoring) vertex to the weight $wt(h)$ is given by u_x (resp. v_x) as defined by (4), and this value is the number of SE (resp. NE) edges to its left, it follows that also

$$(34) \qquad wt(h) = \sum_{x=1}^{\infty} w_x.$$

As in Section 4.4, we first consider the case where $a = b$, and match each path segment of h^{cut} with another at the same height, one NE and one SE (the order is immaterial). If they extend between vertices $(x - 1, h_x^{\mathrm{cut}} - 1)$ and (x, h_x^{cut}), and vertices $(x' - 1, h_x^{\mathrm{cut}})$ and $(x', h_x^{\mathrm{cut}} - 1)$ respectively, then in (34), together they contribute $w_x + w_{x'}$ to $wt(h)$. Let, through the above association, the corresponding straight vertices of $\hat{h}^{\mathrm{cut}}$ be $(\hat{x}, \hat{h}_{\hat{x}}^{\mathrm{cut}})$ and $(\hat{x}', \hat{h}_{\hat{x}}^{\mathrm{cut}})$ (they are at the same height), and let their coordinates in the system (32) be $(\hat{u}_{\hat{x}}, \hat{v}_{\hat{x}})$ and $(\hat{u}'_{\hat{x}'}, \hat{v}'_{\hat{x}'})$ respectively. Then the above association implies that $w_x = \hat{v}_{\hat{x}}$ and $w_{x'} = \hat{u}'_{\hat{x}'}$, and therefore

$$(35) \qquad w_x + w_{x'} = \hat{v}_{\hat{x}} + \hat{u}'_{\hat{x}'} = \frac{1}{2}(\hat{x} + \hat{x}').$$

Since this is the contribution of these two straight vertices to $\hat{w}^{\circ}(\hat{h}^{\mathrm{cut}})$ using (8), we conclude that $\hat{w}^{\circ}(\hat{h}^{\mathrm{cut}}) = wt(h^{\mathrm{cut}})$. But $\widehat{wt}(\hat{h}^{\mathrm{cut}}) = \hat{w}^{\circ}(\hat{h}^{\mathrm{cut}})$ for $a = b$, thereby proving that $\widehat{wt}(\hat{h}^{\mathrm{cut}}) = wt(h^{\mathrm{cut}})$ in this $a = b$ case.

In the $a \neq b$ case, proceed by extending the truncated h^{cut} to the right from $(L(h^{\mathrm{cut}}), b)$ to $(L(h^{\mathrm{cut}}) + |a - b|, a)$, so that this extended path begins and ends at the same height. Then match the edges of this extended path as before, but do not alter the values of w_x obtained from (33) for h^{cut}, where, in particular, $w_x = 0$ for $x > L(h^{\mathrm{cut}})$.

After flipping this extended path horizontally, shrinking by a factor of 2, and heightening each peak by $1/2$ unit, we obtain the truncated $\hat{h}^{\mathrm{cut}}$, but extended to the left of the vertical axis by $|\hat{a} - \hat{b}|$ units, as in the case of the path in Fig. 3.

If the two matched edges from h^{cut} are both to the left of the extended portion, proceeding as in the $a = b$ case above again yields (35). If one of the two matched edges is in the extended portion, then the corresponding straight vertex is in the extended portion of $\hat{h}^{\mathrm{cut}}$. Then, if x, x', $\hat{x}$, $\hat{x}'$, $(\hat{u}_{\hat{x}}, \hat{v}_{\hat{x}})$ and $(\hat{u}'_{\hat{x}'}, \hat{v}'_{\hat{x}'})$ are obtained as above, either $x > L(h^{\mathrm{cut}})$ whereupon $w_x = 0$ and the definition (32) gives $\hat{v}_{\hat{x}} = 0$, or $x' > L(h^{\mathrm{cut}})$ whereupon $w_{x'} = 0$ and the definition (32) gives $\hat{u}'_{\hat{x}'} = 0$. Thus, (35) also holds in these cases.

Then, in view of (35), we see that sum (34) for $wt(h^{\mathrm{cut}})$ is equal to half the sum over the values of $\hat{x}$ of the straight vertices of the extended half-lattice path $\hat{h}^{\mathrm{cut}}$. Through the trick of Section 3.3, this sum gives $\widehat{wt}(\hat{h}^{\mathrm{cut}})$, and therefore $\widehat{wt}(\hat{h}^{\mathrm{cut}}) = wt(h^{\mathrm{cut}})$ in this $a \neq b$ case.

5.5. Proof of $\mathcal{M}(p, 2p - 1)$ weight preservation (iii).

On numbering the peaks of $\hat{h}^{\mathrm{cut}}$ from the left, the half-lattice path $\hat{h}^{\mathrm{int}}$ is obtained from $\hat{h}^{\mathrm{cut}}$ by raising each of the peaks numbered $\mu_1, \mu_2, \ldots, \mu_c$ by inserting a NE-SE edge pair. This is exactly the process examined in Section 4.5. Therefore, from (25), we immediately obtain

$$(36) \qquad \widehat{wt}(\hat{h}^{\mathrm{int}}) = \widehat{wt}(\hat{h}^{\mathrm{cut}}) + \frac{c}{2}(\ell + c - 1) + \sum_{i=1}^{c} \mu_i,$$

where ℓ is the number of straight vertices in $\hat{h}^{\mathrm{cut}}$.

5.6. **Proof of** $\mathcal{M}(p, 2p-1)$ **weight preservation (iv).** Consider the insertion of a NE-SE edge pair at a vertex of a half-lattice path which is either a valley or straight. If it is a valley or straight-up, and there are i straight vertices to its right, the insertion moves each of these straight vertices one unit to the right, resulting, via (8), in a weight increase of $i/2$. If it is a straight-down vertex, and there are $i-1$ straight vertices to its right, the insertion moves each of these straight vertices as well as the straight-down vertex itself one unit to the right, thus also resulting in a weight increase of $i/2$.

With the accretion vertices of $\hat{h}^{\mathrm{int}}$ numbered from the right, the specification of their positions ensures that the jth, if a valley or a straight-up vertex, has exactly $2j$ straight vertices to its right, and if straight-down, has exactly $2j-1$ straight vertices to its right.

Thus, since the half-lattice path $\hat{h}$ is obtained from $\hat{h}^{\mathrm{int}}$ by inserting NE-SE edge pairs at the accretion vertices numbered $\nu_1, \nu_2, \ldots, \nu_d$ (some of which may be equal), we obtain

$$(37) \qquad \widehat{wt}(\hat{h}) = \widehat{wt}(\hat{h}^{\mathrm{int}}) + \sum_{i=1}^{d} \nu_i.$$

5.7. **Proof of** $\mathcal{M}(p, 2p-1)$ **weight preservation (v).** We claim that ℓ, the number of straight vertices in $\hat{h}^{\mathrm{cut}}$, is given by $\ell = 2k - 2m$. To see this, consider the association between the lines of h^{cut} and $\hat{h}^{\mathrm{cut}}$ described in the second paragraph of Section 5.4.

If the truncated h^{cut} has m peaks, let the lengths of the lines to the left and right of the ith peak be $2k_i^L - 1$ and $2k_i^R - 1$, for $1 \le i \le m$. Altogether, these lines contain $k_1^L + \cdots + k_m^L + k_1^R + \cdots + k_m^R$ scoring vertices. The corresponding lines in $\hat{h}^{\mathrm{cut}}$ then contain $2(k_1^L + \cdots + k_m^L + k_1^R + \cdots + k_m^R) - 2m$ straight vertices. This proves the claim when the first and last lines of the truncated h^{cut} are in the NE and SE directions respectively.

If the first line is in the SE direction and is of length $2k_0^R$, then h^{cut} has an additional k_0^R scoring vertices, and $\hat{h}^{\mathrm{cut}}$ has an additional $2k_0^R$ straight vertices (including that at $(0, \hat{a})$). The claim then follows in this case as well.

Likewise, if the last line of the truncated h^{cut} is in the NE direction and is of length $2k_0^L$, then h^{cut} has an additional k_0^L scoring vertices, and $\hat{h}^{\mathrm{cut}}$ has an additional $2k_0^L$ straight vertices. It follows that the claim holds in all cases.

Using (31), (36) and (37), and the fact that $\widehat{wt}(\hat{h}^{\mathrm{cut}}) = wt(h^{\mathrm{cut}})$, we now obtain

$$
\begin{aligned}
(38) \quad \widehat{wt}(\hat{h}) - wt(h) &= \sum_{i=1}^{d} \nu_i + \frac{c}{2}(2k - 2m + c - 1) + \sum_{i=1}^{c} \mu_i - \sum_{i=1}^{n} \lambda_i \\
&= c(k-m) + \frac{c}{2}(c-1) + \sum_{i=1}^{c} \mu_i - \sum_{i=1}^{c} \lambda_i \\
&= 0,
\end{aligned}
$$

having used (29), and where the final equality follows from (28) because

$$(39) \qquad \sum_{i=1}^{c} \lambda_i - \sum_{i=1}^{c} \mu_i = c(k-m) + \sum_{i=0}^{c-1} i = c(k-m) + \frac{1}{2}c(c-1).$$

Thus the weight-preserving nature of the bijection (30) has been proved.

6. Particles in half-lattice paths and fermionic expressions

6.1. **Fermionic expressions.** Here, we derive fermionic expressions for the Virasoro characters $\chi_{r,s}^{p,2p+1}$ and $\chi_{r,s}^{p,2p-1}$ for the cases $r = 1$ and $s = 2$.

Theorem 2. *For $t \in \frac{1}{2}\mathbb{Z}$,*

$$(40) \qquad \chi_{1,2}^{t,2t+1} \equiv \chi_{1,2}^{t+1/2,2t} = \sum_{\boldsymbol{n} \in \mathbb{Z}_{\ge 0}^{2t-3}} \frac{q^{\frac{1}{2}\boldsymbol{n}\boldsymbol{B}^{(t)}\boldsymbol{n}^T}}{(q)_{m_1}} \prod_{j=2}^{2t-3} \begin{bmatrix} n_j + m_j \\ n_j \end{bmatrix}_q,$$

where the sum is over vectors $\boldsymbol{n} = (n_2, n_3, n_4, \ldots, n_{2t-2})$, $\boldsymbol{B}^{(t)}$ *is the* $(2t - 3) \times (2t - 3)$
symmetric matrix defined by

$$(41) \qquad \boldsymbol{B}_{ij}^{(t)} = (i - 1)j \qquad for \ i \leq j, \quad i, j \in \{2, 3, 4, \ldots, 2t - 2\}$$

$(\boldsymbol{B}^{(t)}$ *is the inverse of the Cartan matrix of type* $A_{2t-3})$, *and*

$$(42) \qquad m_d = \sum_{k=d+1}^{2t-2} n_k(k - d), \qquad for \ d \in \{1, 2, 3, \ldots, 2t - 3\}.$$

By virtue of Theorem 1, this may be proved by deriving fermionic expressions for the generating functions $Y_{1,1}^t(q)$ for half-lattice paths. We accomplish this below by applying the method that was developed in [21] (extending that of [8]) to obtain fermionic expressions for the ABF paths. Its applicability relies on $\widehat{wt}(\hat{h})$ being a multiple of the sum of the x-positions of the straight vertices of $\hat{h}$.

6.2. **Identifying particles.** To prove Theorem 2, we first dissect each half-lattice path $\hat{h} \in \mathcal{H}_{1,1}^t$ into particles of various charges as follows (these particles are not related to the particles described in the bijections of Sections 4 and 5). We assign each peak of $\hat{h}$ a charge $\hat{d} \in \{1/2, 1, 3/2, 2, \ldots, t - 1\}$, and associate a particle of that charge with the peak. This is done recursively starting with the peaks of charge $1/2$. Scanning from the right, identify the vertical distances from the peak to the two neighbouring valleys. The peak is assigned a charge $1/2$ if either of those distances is $1/2$. To delineate the particle, a horizontal *baseline* of length 1 is then drawn symmetrically about the peak at a height $1/2$ less than the peak. This baseline will intersect the path twice, with at least one intersection at a valley. In proceeding from the right, a single valley on a baseline is discounted from further consideration (if two, discount only one). Thus, in Fig. 13 for example, having assigned the peak $(45/2, 7/2)$ a charge $1/2$, and drawn its baseline, the valley $(22, 4)$ cannot be used to identify the peak $(43/2, 7/2)$ as charge $1/2$. In this case, the neighbouring valleys are now $(20, 2)$ and $(25, 1)$.

Because of the infinite tail, there will be an infinite number of peaks, and thus particles, of charge $1/2$. The remaining finite number of peaks are then identified with particles of greater charge. Having identified all the peaks having charge $1/2$, we then scan from the right for peaks having vertical distance 1 to one of their neighbouring two valleys, ignoring those valleys discounted previously. For each such peak, we draw a horizontal baseline at a height 1 less than that of the peak, below the peak, extending from the identified valley to where it next intersects the path. These identify the particles of charge 1. Then, continuing in this fashion, next considering charges $\hat{d} = 3/2, 2, 5/2, \ldots, t - 1$, in turn, we eventually assign a charge and a particle to each peak, with its baseline of length $2\hat{d}$ at height $\hat{d}$ below that of the peak. We define the *origin* of the particle to be the position of the left end of its baseline. Note that the baselines are necessarily all at integer heights. The slope of a particle is defined to be that portion of the path that lies above its baseline, but not above other baselines.

This dissection process has been carried out for the path given in Fig. 13. From left to right, its peaks have been assigned charges $\frac{1}{2}, \frac{7}{2}, 1, 2, 1, \frac{5}{2}, \frac{3}{2}, \frac{1}{2}, \frac{1}{2}, \frac{1}{2}, \ldots$.

Although enacted differently to the dissection process described in [21, Section 3.1], the two processes are equivalent.

For $\boldsymbol{n} = (n_2, n_3, n_4, \ldots, n_{2t-2})$, define $\mathcal{H}^{\boldsymbol{n}} \subset \mathcal{H}_{1,1}^t$ to be the set of half-lattice paths that contain n_d particles of charge $d/2$, for $2 \leq d \leq 2t - 2$. Then define $\hat{h}^{\boldsymbol{n}} \in \mathcal{H}^{\boldsymbol{n}}$ to be that element that has minimal weight amongst all the elements of $\mathcal{H}^{\boldsymbol{n}}$. By considering the possible positions of the straight vertices in $\hat{h}^{\boldsymbol{n}}$, it can be seen that the minimal weight condition implies that $\hat{h}^{\boldsymbol{n}}$ is unique, that the baseline of each of the particles in $\hat{h}^{\boldsymbol{n}}$ lies at height 1, and each particle is to the left of all particles of lesser charge. For example, for $\boldsymbol{n} = (2, 1, 1, 1, 0, 1, 0)$, the minimal weight path $\hat{h}^{\boldsymbol{n}} \in \mathcal{H}_{1,1}^5$ is given in Fig. 14.

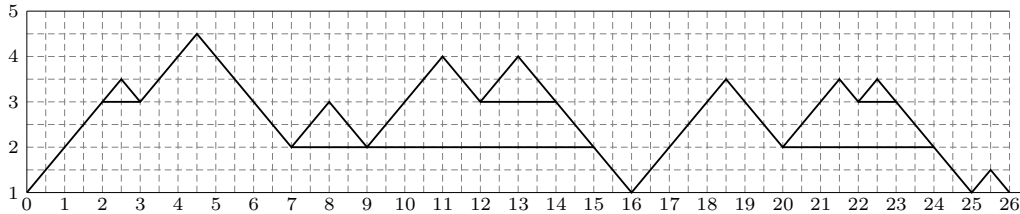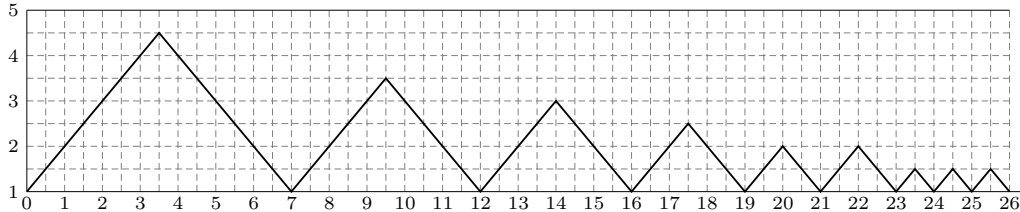FIGURE 13. Dissecting a half-lattice path into particles

FIGURE 14. Minimal weight path $\hat{h}^{(2,1,1,1,0,1,0)} \in \mathcal{H}_{1,1}^5$

Lemma 6.1. *Let $t \in \frac{1}{2}\mathbb{Z}_{\geq 4}$ and $\boldsymbol{n} = (n_2, n_3, n_4, \ldots, n_{2t-2})$. Then, with $\boldsymbol{B}^{(t)}$ given by (41),*

$$\widehat{wt}(\hat{h}^{\boldsymbol{n}}) = \frac{1}{2}\boldsymbol{n}\boldsymbol{B}^{(t)}\boldsymbol{n}^T. \tag{43}$$

Proof: First note that if a particle of charge $d/2$ has its origin at (x, h_x), then its $2(d-1)$ straight vertices contribute

$$\begin{aligned}
\tfrac{1}{2}\big((x + \tfrac{1}{2}) &+ (x + 1) + (x + \tfrac{3}{2}) + \cdots + (x + \tfrac{d}{2} - \tfrac{1}{2}) + (x + \tfrac{d}{2} + \tfrac{1}{2}) + (x + \tfrac{d}{2} + 1) \\
&+ (x + \tfrac{d}{2} + \tfrac{3}{2}) + \cdots + (x + d - \tfrac{1}{2})\big) = (x + \tfrac{d}{2})(d - 1)
\end{aligned} \tag{44}$$

to $\widehat{wt}(\hat{h}^{\boldsymbol{n}})$. Then, a succession of n_d particles of charge $d/2$, with the origin of the first at (x, h_x), contribute

$$\sum_{i=1}^{n_d}(x + (i - \tfrac{1}{2})d)(d - 1) = n_d(x + \tfrac{1}{2}dn_d)(d - 1) \tag{45}$$

to $\widehat{wt}(\hat{h}^{\boldsymbol{n}})$. Now note that the total length of the baselines of the particles of charges $t - 1, t - \frac{3}{2}, t - 2, \ldots, \frac{1}{2}(d + 1)$ is $x = \sum_{j=d+1}^{2t-2} jn_j$. After substituting this into (45), and summing over $d = 2, 3, 4, \ldots, 2t - 2$, expression (43) results. $\qquad\square$

6.3. **Particle moves.** Here we describe a process in which the particles in a path $\hat{h}$ may move. As we will see below, all paths in sector $\mathcal{H}^{\boldsymbol{n}}$ may be generated from the minimal weight path $\hat{h}^{\boldsymbol{n}}$, through this process.

A particle of charge $\hat{d}$ has a permitted move if its baseline has length exactly $2\hat{d}$, and its origin intersects the slope of a particle of greater charge $\hat{d}' > \hat{d}$. Let the peaks of these two particles be at $(x, \hat{h}_x)$ and $(x', \hat{h}_{x'})$ respectively. Note that the restriction that valleys are at integer height implies that $\hat{h}_{x'} - \hat{h}_x$ is an integer if and only if $\hat{d}' - \hat{d}$ is an integer.

If $x < x'$ or $\hat{h}_x \leq \hat{h}_{x'} - 1$ then the move is performed by removing the two edges immediately to the left of the particle of charge $\hat{d}$ (these are necessarily in the same direction), then moving the particle itself two half-units to the left, and two half-units either up or down, to fill the gap, before finally, reinserting the originally removed two edges at the right of the particle to recover a connected path. This process has been carried out for the first, second and fourth moves illustrated in Fig. 15.

FIGURE 15. Move sequence for $c = 3/2$, $c' = 7/2$.
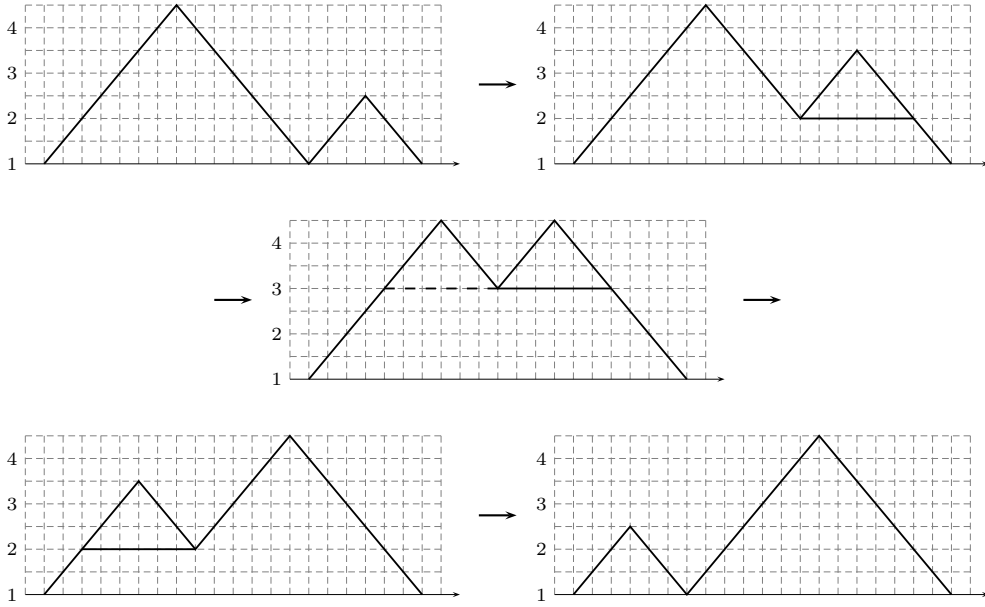
If $x > x'$ and $\hat{h}_x = \hat{h}_{x'}$ then this same procedure is carried out after, contrary to the above convention, considering the peak at $(x', \hat{h}_{x'})$ to be that of the particle of charge $\hat{d}$, and the peak at $(x, \hat{h}_x)$ that of the particle of change $\hat{d}'$. The baseline of the former is moved accordingly. For example, in the third path picture of Fig. 15, the original definition associates particles of charges $7/2$ and $3/2$ with the two peaks. The baseline of the latter is shown as a solid line. Before enacting its move, we first reassign the first peak as that having a charge $3/2$, with the dashed line as its baseline. The move then results in the fourth path.

If $x > x'$ and $\hat{h}_{x'} = \hat{h}_x + \frac{1}{2}$, then necessarily $x = x' + 2\hat{d} + \frac{1}{2}$. The move is then enacted by lowering the peak at $(x', \hat{h}_{x'})$ by $1/2$ unit by removing a NE-SE edge pair, and heightening the peak at $(x, \hat{h}_x)$ by inserting a NE-SE pair. This results in peaks at $(x' - \frac{1}{2}, \hat{h}_{x'} - \frac{1}{2})$ and $(x - \frac{1}{2}, \hat{h}_x + \frac{1}{2})$, with the former now associated with the particle of charge $\hat{d}$. This move is illustrated by the transition between the second and third paths in Fig. 16. (Note that this latter move may be regarded as two half-moves of the above types.)

FIGURE 16. Move sequence for $\hat{d} = 3/2$, $\hat{d}' = 3$.
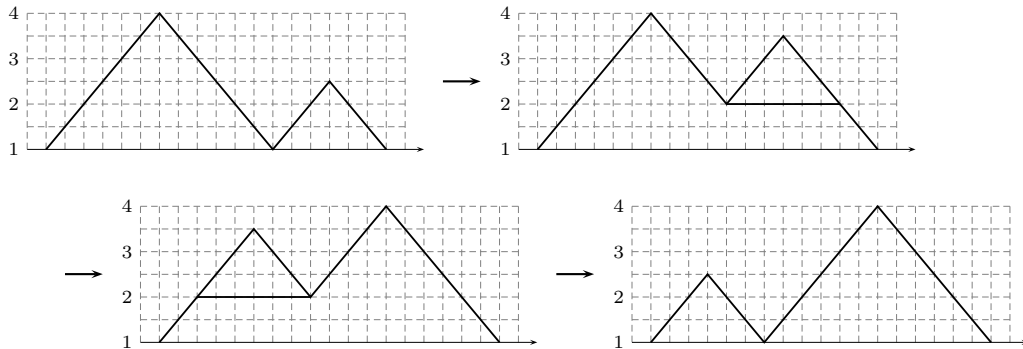
Lemma 6.2. *Let $\hat{h}'$ be obtained from $\hat{h} \in \mathcal{H}_{1,1}^t$ using one of the above moves. Then*

$$(46) \qquad \widehat{wt}(\hat{h}') = \widehat{wt}(\hat{h}) + 1.$$

Proof: In the first cases, two straight vertices have each moved a distance of $2\hat{d}$ to the right, while the $4\hat{d} - 2$ straight vertices of the particle have each moved a distance of 1 to the left. In view of (8) and (9), we therefore obtain $\widehat{wt}(\hat{h}') - \widehat{wt}(\hat{h}) = \frac{1}{2}(4\hat{d} - (4\hat{d} - 2)) = 1$.

For the last case, the move may be regarded as having the $4\hat{d} - 2$ straight vertices of the particle moving to the left by a distance of $2\hat{d}+1$, with $4\hat{d}$ straight vertices of the other peak moving a distance of $2\hat{d}$ to the right. Then, from (8) and (9), we obtain $\widehat{wt}(\hat{h}') - \widehat{wt}(\hat{h}) = \frac{1}{2}(8\hat{d}^2 - (4\hat{d} - 2)(2\hat{d} + 1)) = 1$. $\qquad\square$

Once a particle has moved using the process described above, it can move again unless its origin is at the path startpoint $(0, 1)$ or lies also on the slope of a particle of equal or lesser charge. However, since the particle's origin shifts to the left with each move, only a finite number of such moves are possible. For a fixed sector $\boldsymbol{n}$, we define m_d to be the maximal number of moves that can be performed on the leftmost particle of charge $d/2$ from $\hat{h}^{\boldsymbol{n}}$ (if there is such a particle). We now claim that m_d, defined in this way, accords with that specified in Theorem 2.

Lemma 6.3.

$$(47) \qquad m_d = \sum_{k=d+1}^{2t-2} n_k(k - d).$$

Proof: In $\hat{h}^{\boldsymbol{n}}$, the baseline of each particle of charge $d'/2$ has length d'. Therefore, the origin of the leftmost particle of charge d is at position $(x, 1)$ where $x = \sum_{k=d+1}^{2t-2} kn_k$. Consider repeatedly moving this particle to the left. Each move of the first type shifts the origin of the particle 1 unit to the left. However, for each of the particles to its left (which have greater charge), one of the other move descriptions must eventually be carried out. For the second type of move, the change in convention for the position of the particle, means that the particle's origin shifts to the left by a distance d before the move is enacted. For the third type of move, the particle's origin shifts to the left by a distance $d + 1$ in carrying out the move. Thus, once we have subtracted from x a contribution of d for each particle of charge greater then d, the number of moves, m_d, required to shift the particle's origin to $(0, 1)$, remains. This yields (47). $\qquad\square$

Lemma 6.4. *For $t \in \frac{1}{2}\mathbb{Z}$ and $\boldsymbol{n} = (n_2, n_3, n_4, \dots, n_{2t-2}) \in \mathbb{Z}_{\geq 0}^{2t-3}$,*

$$(48) \qquad \sum_{\hat{h} \in \mathcal{H}^{\boldsymbol{n}}} q^{\widehat{wt}(\hat{h})} = \frac{q^{\frac{1}{2}\boldsymbol{n}\boldsymbol{B}^{(t)}\boldsymbol{n}^T}}{(q)_{m_1}} \prod_{j=2}^{2t-3} \begin{bmatrix} n_j + m_j \\ n_j \end{bmatrix}_q,$$

where $\boldsymbol{B}^{(t)}$ is defined by (41) and m_d is specified by (42) for $1 \leq d < 2t - 2$.

Proof: Lemma 6.3 shows that the maximal number of moves for the leftmost particle of charge $d/2$ in $\hat{h}^{\boldsymbol{n}}$ is given by m_d. If $\lambda_1^{(d)} \leq m_d$ moves are actually carried out, then we may consider moving the next leftmost particle of charge $d/2$, if there is one. We see that it may move $\lambda_2^{(d)} \leq \lambda_1^{(d)}$ times, because each of its moves is a shifted version of the corresponding move of the other particle, and after $\lambda_1^{(d)}$ moves, it will lie alongside the other, and be unable to move further. Proceeding likewise with each of the n_d particles of charge $d/2$, we find that, altogether, their possible moves are indexed by partitions $\lambda^{(d)} = (\lambda_1^{(d)}, \lambda_2^{(d)}, \dots, \lambda_{n_d}^{(d)})$, with largest part at most m_d. Since, by Lemma 6.2, each move increases the weight of the path by 1, moving the particles of charge $d/2$ in accordance with the parts of the partition $\lambda^{(d)}$ increases the weight by $|\lambda^{(d)}|$, where, as usual, the weight $|\lambda|$ of a partition $\lambda = (\lambda_1, \lambda_2, \dots, \lambda_n)$ is defined by $|\lambda| = \sum_{i=1}^n \lambda_i$.

However, the proof of Lemma 6.3 applies equally if the particles of charges greater than $d/2$ have themselves already been subject to moves. Thus, we may first subject the particles of charge $t - 3/2$ to moves indexed by a partition $\lambda^{(2t-3)}$ having at most n_{2t-3} parts with maximal part m_{2t-3}, followed by subjecting the particles of charge $t-2$ to moves indexed by a partition $\lambda^{(2t-4)}$ having at most n_{2t-4} parts with maximal part m_{2t-4}, and so on, ending with a partition $\lambda^{(1)}$ having an unlimited number of parts (because there are an infinite number of particles of charge $1/2$) but maximal part m_1. The weight of a path obtained through this correspondence is equal to

$$(49) \qquad \widehat{wt}(\hat{h}^{\boldsymbol{n}}) + |\lambda^{(2t-3)}| + |\lambda^{(2t-4)}| + \cdots + |\lambda^{(1)}|.$$

Then, since the generating function for partitions λ with at most n parts with maximal part m is given by [1]

$$(50) \qquad \sum_{\substack{\lambda=(\lambda_1,\lambda_2,...,\lambda_n) \\ m \geq \lambda_1 \geq \lambda_2 \geq \cdots \geq \lambda_n \geq 0}} q^{|\lambda|} = \begin{bmatrix} n + m \\ n \end{bmatrix}_q,$$

and the generating function for partitions λ with an unlimited number of parts but maximal part m is given by

$$(51) \qquad \sum_{\substack{\lambda=(\lambda_1,\lambda_2,...) \\ m \geq \lambda_1 \geq \lambda_2 \geq \cdots \geq 0}} q^{|\lambda|} = \frac{1}{(q)_m},$$

it follows that the generating function for the set of paths obtained by moving the particles of $\hat{h}^{\boldsymbol{n}}$ is given by the right side of (48), having made use of Lemma 6.1.

It remains to show that every element of $\mathcal{H}^{\boldsymbol{n}}$ is obtained by moving the particles of $\hat{h}^{\boldsymbol{n}}$. To see this, for an arbitrary path $\hat{h} \in \mathcal{H}^{\boldsymbol{n}}$, consider first the particles of charge $1/2$ that do not belong to the tail. Starting with the rightmost, these may be moved rightward by a succession of moves reverse to those defined above, until they belong to the tail. We then proceed similarly with the particles of charge 1, starting with the rightmost, and moving it rightward until it is alongside the tail. Continuing in this way in turn for all the particles in $\hat{h}$, we obtain $\hat{h}^{\boldsymbol{n}}$. By inverting this procedure, it is then clear that $\hat{h}$ can be obtained from $\hat{h}^{\boldsymbol{n}}$ by moving its particles. $\qquad \square$

Proof of Theorem 2: Since every path $\hat{h} \in \mathcal{H}^t_{1,1}$ is a member of a unique $\mathcal{H}^{\boldsymbol{n}}$, we obtain

$$(52) \qquad Y^t_{1,1}(q) = \sum_{\boldsymbol{n} \in \mathbb{Z}^{2t-3}_{\geq 0}} \sum_{\hat{h} \in \mathcal{H}^{\boldsymbol{n}}} q^{\widehat{wt}(\hat{h})} = \sum_{\boldsymbol{n} \in \mathbb{Z}^{2t-3}_{\geq 0}} \frac{q^{\frac{1}{2}\boldsymbol{n}\boldsymbol{B}^{(t)}\boldsymbol{n}^T}}{(q)_{m_1}} \prod_{j=2}^{2t-3} \begin{bmatrix} n_j + m_j \\ n_j \end{bmatrix}_q,$$

by summing Lemma 6.4 over all $\boldsymbol{n}$. Theorem 2 then follows from Theorem 1. $\qquad \square$

7. DISCUSSION

In this work, we have demonstrated that half-lattice paths provide a combinatorial model for the $\chi^{p,2p\pm1}_{r,s}$ characters, and give rise to fermionic expressions via techniques used in the ABF cases. These expressions are distinct from the fermionic expressions for these characters obtained previously using the RSOS paths. The existence of these different fermionic expressions can be attributed to the fact that there exist different perturbations of the $\mathcal{M}(p, p')$ conformal field theory that remain solvable away from the critical limit [4, 6]. The RSOS statistical models [2, 14] realise the so-called $\phi_{1,3}$ perturbation. We anticipate that the half-lattice paths correspond to configuration sums of statistical models that realise the $\phi_{1,5}$ perturbation when $p' = 2p + 1$ and the $\phi_{2,1}$ perturbation when $p' = 2p - 1$. The bijections described in this paper would therefore provide a combinatorial connection between these perturbations and the $\phi_{1,3}$ perturbation. However, this connection is not expected to be significant from the physical point of view.

In a forthcoming paper, we obtain novel fermionic expressions for all the generating functions $Y^t_{\hat{a},\hat{b}}(q)$, and thus, through Theorem 1 above, all characters $\chi^{p,2p\pm1}_{r,s}$. We also obtain fermionic expressions for the finitizations of these characters that are the generating functions of finite length half-lattice paths. In fact, in each case, we obtain four fermionic expressions. From a combinatorial point of view, these arise in a way similar to that of Melzer's expressions [19, 12] for the ABF cases.

Appendix A. The Virasoro algebra and the minimal models

A.1. **The Virasoro algebra.** The Virasoro algebra Vir is the infinite-dimensional Lie algebra over $\mathbb{C}$ with basis

$$\{\hat{c}, L_i \,|\, i \in \mathbb{Z}\}, \tag{53}$$

whose elements are subject to the commutation relations

$$[L_n, L_m] = (n-m)L_{n+m} + \frac{1}{12}n(n^2-1)\delta_{n,-m}\hat{c},$$
$$[\hat{c}, L_n] = 0, \tag{54}$$

for all $m, n \in \mathbb{Z}$.

A.2. **Highest weight modules.** For $c, \Delta \in \mathbb{C}$, a highest weight module $V_{c,\Delta}$ of Vir is a module of Vir that is generated by a vector $v \in V_{c,\Delta}$, for which

$$L_n\, v = 0 \text{ for all } n > 0,$$
$$\hat{c}\, v = c\, v, \tag{55}$$
$$L_0\, v = \Delta\, v.$$

The (normalised) character $\chi(V)$ of a highest weight module V is a q-series in which the coefficient of q^n is the dimension of the eigenspace of V, on which L_0 has eigenvalue $\Delta + n$. Formally,

$$\chi(V) = q^{-\Delta}\,\mathrm{Tr}_V\, q^{L_0}. \tag{56}$$

A.3. **Verma module.** Let $M_{c,\Delta}$ denote the Verma module of Vir that has a highest weight vector v satisfying (55). The commutation relations in Vir imply that $M_{c,\Delta}$ has a basis comprising all vectors of the form

$$L_{-n_1}L_{-n_2}L_{-n_3}\cdots L_{-n_k}\, v, \tag{57}$$

with $n_1 \geq n_2 \geq n_3 \geq \cdots \geq n_k > 0$.

Note that (54) implies that

$$L_0(L_{-n_1}L_{-n_2}L_{-n_3}\cdots L_{-n_k}\, v) = (n+\Delta)(L_{-n_1}L_{-n_2}L_{-n_3}\cdots L_{-n_k}\, v), \tag{58}$$

where $n = n_1 + n_2 + \cdots + n_k$. It follows that $\chi(M_{c,\Delta})$ is the "partition generating function":

$$\chi(M_{c,\Delta}) = \frac{1}{(q)_\infty}. \tag{59}$$

A.4. **Minimal model Virasoro characters.** For generic values of c and Δ, the Verma module $M_{c,\Delta}$ is irreducible. The non-generic cases where c is rational are especially important in physics. These cases are usually parameterised by four integers p, p', r, s for which p and p' are coprime with $1 < p < p'$, and $1 \leq r < p$ and $1 \leq s < p'$ [17, 10]. Here

$$c = 1 - 6\frac{(p'-p)^2}{pp'} \quad\text{and}\quad \Delta = \frac{(p'r-ps)^2 - (p'-p)^2}{4pp'}. \tag{60}$$

In these cases, the Verma module $M_{c,\Delta}$ is reducible and its irreducible quotient has character given by (1) [20]. The expression (1) is known as a bosonic expression because it arises on formulating the Verma module as a bosonic Fock space, from which submodules are then factored out. Such expressions are thus the difference of two (genuine) q-series.

It is useful to note the following identities which are obtained directly from (1):

$$\chi_{r,s}^{p,p'} = \chi_{p-r,p'-s}^{p,p'},$$
(61)

$$\chi_{r,s}^{p,p'} = \chi_{s,r}^{p',p} = \chi_{s/k,kr}^{p'/k,kp},$$
(62)

regardless of whether $kp, kr, p'/k, s/k$ are integers.

We will understand here that the "Minimal Model" $\mathcal{M}(p,p')$ is the direct sum of all irreducible modules $V_{c,\Delta}$ for c and Δ obtained from (60) as r and s run over their ranges $1 \leq r < p$ and $1 \leq s < p'$.

REFERENCES

[1] G.E. Andrews, *The Theory of Partitions*, Encyclopedia of Mathematics and its Applications, Vol. 2 (Addison-Wesley, Reading, MA), 1976.

[2] G.E. Andrews, R.J. Baxter and P.J. Forrester, *Eight-vertex SOS model and generalized Rogers-Ramanujan-type identities*, J. Stat. Phys. **35** (1984) 193–266.

[3] A. Berkovich and B.M. McCoy, *Continued fractions and fermionic representations for characters of $\mathcal{M}(p,p')$ minimal models*, Lett. Math. Phys. **37** (1996) 49–66.

[4] A. Berkovich and B.M. McCoy, *Rogers-Ramanujan identities: A century of progress from mathematics to physics*, Doc. Math. J. DMV, Extra Volume ICM III (1998) 163–172.

[5] A. Berkovich, B.M. McCoy and A. Schilling, *Rogers-Schur-Ramanujan type identities for the $M(p,p')$ minimal models of conformal field theory*, Commun. Math. Phys. **191** (1998) 325–395.

[6] A. Berkovich, B.M. McCoy and P.A. Pearce, *The perturbations $\phi_{2,1}$ and $\phi_{1,5}$ of the minimal models $M(p.p')$ and the trinomial analogue of Bailey's lemma*, Nucl. Phys. **B519** (1998) 597–625.

[7] O. Blondeau-Fournier, P. Mathieu and T.A. Welsh, *A bijection between paths for the $M(p, 2p+1)$ minimal model Virasoro characters*, Ann. Henri Poincaré **11** (2010) 101–125.

[8] D.M. Bressoud, *Lattice paths and the Rogers-Ramanujan identities* in "Proceedings of the International Ramanujan Centenary Conference, 1987 Madras", ed. K. Alladi, Lecture Notes in Mathematics **1395** (Springer, New York), 1989, pp. 140–172.

[9] E. Date, M. Jimbo, A. Kuniba, T. Miwa and M. Okado, *Exactly solvable SOS models: local height probabilities and theta function identities*, Nucl. Phys. **B290** (1987) 231–273.

[10] P. Di Francesco, P. Mathieu and D. Sénéchal, *Conformal Field Theory* (Springer-Verlag, New York), 1997.

[11] O. Foda, K.S.M. Lee, Y. Pugai and T.A. Welsh, *Path generating transforms*, Contemp. Math. **254** (2000) 157–186.

[12] O. Foda and T.A. Welsh, *Melzer's identities revisited*, Contemp. Math. **248** (1999) 207–234.

[13] O. Foda and T.A. Welsh, *On the combinatorics of Forrester-Baxter models*, in proceedings of "Physical Combinatorics", Kyoto 1999, eds. M. Kashiwara and T. Miwa, Prog. Math. **191** (Birkhäuser, Boston), 2000, pp. 49–103.

[14] P.J. Forrester and R.J. Baxter, *Further exact solutions of the eight-vertex SOS model and generalizations of the Rogers-Ramanujan identities*, J. Stat. Phys. **38** (1985) 435–472.

[15] P. Jacob and P. Mathieu, *A new path description for the $\mathcal{M}(k+1, 2k+3)$ models and the dual $\mathcal{Z}_k$ graded parafermions*, J. Stat. Mech. (2007) P11005 (43 pp).

[16] P. Jacob and P. Mathieu, *Particles in RSOS paths*, J. Phys. A **42** (2009) 122001 (14 pp).

[17] V. Kac and A.K. Raina, *Bombay lectures on highest weight representations of infinite dimensional Lie algebras* (World Scientific, Singapore), 1987.

[18] R. Kedem, T.R. Klassen, B.M. McCoy and E. Melzer, *Fermionic sum representations for conformal field theory characters*, Phys. Lett. B **307** (1993) 68–76.

[19] E. Melzer, *Fermionic character sums and the corner transfer matrix*, Int. J. Mod. Phys. **A9** (1994) 1115–1136.

[20] A. Rocha-Caridi, *Vacuum vector representations of the Virasoro algebra*, in proceedings of "Vertex Operators in Mathematics and Physics", eds. J. Lepowsky et al. (Springer-Verlag, New York), 1985, pp. 451–473.

[21] S.O. Warnaar, *Fermionic solution of the Andrews-Baxter-Forrester model. I. Unification of CTM and TBA methods*, J. Stat. Phys. **82** (1996) 657–685.

[22] S.O. Warnaar, *Fermionic solution of the Andrews-Baxter-Forrester model. II. Proof of Melzer's polynomial identities*, J. Stat. Phys. **84** (1996), 49–83.

[23] S.O. Warnaar, *q-Trinomial identities*, J. Math. Phys. **40** (1999) 2514–2530.

[24] T.A. Welsh, *Fermionic expressions for minimal model Virasoro characters*, Mem. Amer. Math. Soc. **175** (no. 827) 2005.

Département de physique, de génie physique et d'optique, Université Laval, Québec, Canada, G1K 7P4.

E-mail address: `olivier.b-fournier.1@ulaval.ca`

Département de physique, de génie physique et d'optique, Université Laval, Québec, Canada, G1K 7P4.

E-mail address: `pmathieu@phy.ulaval.ca`

Département de physique, de génie physique et d'optique, Université Laval, Québec, Canada, G1K 7P4; and Department of Physics, University of Toronto, Ontario, Canada, M5S 1A7.

E-mail address: `trevor.welsh@utoronto.ca`